ARTIFICIAL SATELLITES, Vol. 50, No. 2 – 2015
DOI: 10.1515/arsa-2015-0006

IMPACT OF OCEAN TIDES LOADING ON PRECISE POINT POSITIONING BASED ON FES2004 MODEL

J. Z. Kalita[1)], Z. Rzepecka[2)]
[1)] Department of Civil Engineering, Environmental Engineering and Geodesy, Koszalin University of Technology
[2)] Institute of Geodesy, University of Warmia and Mazury in Olsztyn
e-mails: jakub.kalita@tu.koszalin.pl, zofia.rzepecka@uwm.edu.pl

ABSTRACT.
Precise Point Positioning (PPP) technique as an absolute positioning method requires modeling of effects that influence observations. One of the effects is a displacement of the measurement location due to ocean mass gravitational attraction - ocean tides loading (OTL). The model recommended by the International Earth Rotation and Reference Systems Service (IERS) is FES2004. The paper focuses on impact of applying the particular OTL model on PPP processing. The analysis is based on processing of observations from 24 globally distributed permanent stations and time span of 50 days. The analysis bases on processing intervals from 1 to 24 hours. In addition, the amplitudes of the loads in Poland are evaluated. The OTL model is location dependent, thus the importance of applying this model depends on the location environment. As the PPP is an absolute method, the loads cumulate and transfer nearly directly to the positioning solution. Consequently, for short observation intervals and small loads the application of the model does not play an important role. For the analysed station with high amplitudes of the loads the relative and absolute improvement, of the solution was the highest for height component. By applying the model, the solution improved by 19% or 7.3 mm (as for RMS and 8 hour interval). The distinct improvement for convergence exists for vertical component and threshold below 5 cm. For Poland the vertical component loads were about 5 times smaller and the highest improvement for the analysed station was 3.7% for 4 hour interval and vertical component.

Keywords: Ocean Tides Loading, FES2004, Precise Point Positioning.

1. INTRODUCTION

Precise Point Positioning (PPP) is an absolute positioning method based on Global Navigation Satellite System (GNSS). Its intensive development reaches the 90s (Zumberge et al, 1997). With single receiver required for the positioning using this method, the coverage is homogenous globally. This contrasts with relative methods that depend on distances to reference stations.

Precise satellite positions and satellite clock corrections are crucial for positioning quality. One of the ephemeris data sources is the International GNSS Service (IGS). It provides data with several precision levels. The most precise set is based on weighted linear combination of

data from several analysis centers. The orbits are precise to 1-2 cm. The clocks precision is 20-60 picoseconds (Kouba, 2009; Griffiths and Ray, 2009). The IGS claims precision of 2.5 cm and 75 picoseconds for orbits and clocks respectively, with respective intervals of 15 minutes and 30 seconds (Kouba, 2009).The ephemeris define the coordinate reference system of the result coordinates. In case of using the IGS orbits the PPP solutions are directly in the IGS global reference frame which conforms to the ITRF (Kouba, 2009).

PPP as an absolute method should include models for additional effects that influence the signal. Among them are the following: special and general relativity, Sagnac delay, satellite antenna and clock offsets, phase wind-up, solid earth tides, ocean loading, Earth rotation parameters and atmospheric pressure loading (Kouba and Heroux, 2001; Hofmann-Wellenhof et al., 2008). Including the above effects, the observation equations can be defined as follows:

$$l_{P_i} = \rho + cd_t - cd^T + d_{trop} + d_{ion_{Pi}} + \Delta + \varepsilon_{P_i} \tag{1}$$

$$l_{\Phi_i} = \rho + cd_t - cd^T + \lambda(N + B + b) + d_{trop} - d_{ion_{\Phi i}} + \Delta + \varepsilon_{\Phi_i} \tag{2}$$

$$\Delta = d_{phc} + d_{rel} + d_{grav} + d_{wup} + d_{s\_tides} + d_{o\_tides} \tag{3}$$

where:

l_{P_i}, l_{Φ_i}	are pseudo-ranges and carrier-phases, respectively for frequency *i* [m]
ρ	geometrical distance between the receiver antenna and the satellite [m]
d_t, d^T	station and satellite clock offsets from GPS time [s]
c	speed of light in a vacuum [m/s]
d_{trop}	signal path delay due to propagation through neutral atmosphere [m]
$d_{ion_{P_i}}, d_{ion_{\Phi_i}}$	signal path delay due to propagation through ionosphere for frequency *i* [m]
N	ambiguity parameter for the phase observation [cycle]
B, b	uncalibrated phase delays for receiver and satellite, respectively [cycle]
λ	wavelength for carrier-phase respective frequency [m]
$\varepsilon_{P_i}, \varepsilon_{\Phi_i}$	measurement noise for pseudo-range and carrier-phase, respectively [m]
Δ	correction component containing satellite and receiver phase centers d_{phc}, relativistic d_{rel} and gravitational d_{grav} effects, wind-up effect d_{wup}, effects of solid d_{s_tides} and ocean d_{o_tides} tides loading[m]

After correcting the observations using satellite precise clock corrections and antenna phase center variations and removing the effects by appropriate models, the influence of ionosphere may be reduced by using ionosphere-free linear combination of dual frequency observations. The observation equations can be defined as (Kouba and Heroux, 2001):

$$l_{P_{IF}} = \rho + cd_t + d_{trop} + \varepsilon_{P_{IF}} \tag{4}$$

$$l_{\Phi_{IF}} = \rho + cd_t + d_{trop} + N_{IF}\lambda_{IF} + \varepsilon_{\Phi_{IF}} \tag{5}$$

where the *IF* subscript stands for ionosphere free linear combination. The noise component contains all additional effects not handled in the observation equations.

The model presented in Eqs. 1 and 2 can be solved using either sequential least squares adjustment or Kalman filtering (cf. Kouba and Heroux, 2001; Hofmann-Wellenhof et al., 2008; Leandro et al. 2011; Stępniak et al., 2012).

For static positioning the PPP solution converges to centimeter level (cf. Abdel-Salam, 2005; Ebner and Featherstone, 2008; Bisnath and Gao, 2009; Kouba, 2009; Landau et al.,

2009;Leandro et al., 2011; Stępniak et al., 2012).Time needed for the mentioned quality varies between 12 and 24 hours depending on satellites' geometry and station specific environment conditions (Bisnath and Gao, 2009).Decimeter level accuracy is obtained during first hour of observation. The nature of convergence threshold in observation length is exponential with high variability even for single stations (Bisnath and Gao, 2009; Kalita et al., 2014).

2. OCEAN TIDES LOADING

The cause of tides are forces exerted by gravitational attraction between the Earth and astronomical masses located in the Earth's vicinity. The influence may be described by the concept of gravitational potential, a scalar value, which gradient is a force generated at particular point. Total potential is a sum of potentials generated by each mass according to superposition principle. Tide generating potential for the Earth may be composed of the sum of harmonics (Dodson, 1921; IERS Conventions, 2010)

One of reactions for change of the Earth's gravity potential field due to orbital motions of celestial bodies are ocean tides. The most significant influence is generated by the Moon and the Sun. The tides are strongly influenced by local factors and thus tide models are based on grids covering the ocean surface (IERS Conventions, 2010).

OTL is generated by tidal oceans mass distribution variations. It can be calculated as a convolution of the ocean tides model with point surface load, which in turn can be described by Green function (Farrel, 1972). Integration over global ocean results in final displacement of a particular point due to the ocean tides.

In practice, the procedure for calculating the displacements should base on the most recent ocean tides models, one of which is the FES2004 (Finite Element Solution). The FES2004 ocean atlas was computed using the CEFMO hydrodynamic model (Code aux Eléments Finis pour la Marée Oceanique) with the CADOR (Code d'Assimilation de Données Orienté Représenteur) method for assimilating tide gauge and altimeter data (Lyard et al., 2006). Grid resolution is 0.125 degree (IERS Conventions, 2010).It uses finite element mesh named Global Finite Element Model-2 (GFEM-2), designed so that elements length is proportional to local ocean's depth and slope. This enables to take into account coastlines, shelf breaks and volcanic ridges. The mesh results in 500000 elements and 1000000 computational nodes (Lyard et al., 2006).

The loading calculation scheme used in this paper is based on the FES2004 model and IERS's procedure (IERS Conventions, 2010). For particular location,11 pairs of amplitudes and phases, representing the most of the total tidal signal, are obtained (H.-G.Scherneck provides various models including FES2004 at *http://holt.oso.chalmers.se/loading/*). The file is written in a commonly used BLQ format and contains tidal coefficients for 3 long-term (Mf, Mm, Ssa), 4 diurnal (K1, O1, P1, Q1) and 4 semi-diurnal (M2, S2, N2, K2) waves. Sample values for these waves are presented in Table 1. The tidal coefficients can be obtained in respect to a reference system with origin coinciding with the center of mass of the whole Earth system (CM) including ocean and other surface loads such as atmosphere and continental water storage (Blewitt, 2003). In this case the movement of the fluid mass is accompanied by the opposite motion of the center of mass of the solid Earth. An alternative is the center of the Earth (CE) frame which holds fixed the averaged center of mass location of the solid Earth. The IGS preprocessed orbits are in crust-fixed ITRF that is not sensitive to the Earth's center of mass and thus, when using them, ocean loading coefficients should not be corrected for geocenter motion (Kouba, 2009); the CM frame should be used. Fu et al. (2011)

claims that distortions on the level of over a single millimeters can appear when using inconsistent tidal loading models during PPP processing.

Amplitudes and phases of 11 main tides, characteristic to particular location, are input to the HARDISP procedure (the FORTRAN code is available at: *ftp://tai.bipm.org/iers/convupdt/chapter7/hardisp/HARDISP.F*). Final set of 342 constituent tides used in the procedure, recommended by the IERS, is obtained basing on 11 mentioned loading coefficients. The interpolation takes place in complex domain and thus the admittance is obtained for main tides. The real and imaginary parts for all frequencies are obtained using spline interpolation. Afterwards, amplitudes and phases are transformed back from complex domain. The displacement for each component is obtained as a sum for a set of tidal constituents (IERS Conventions, 2010) as follows:

$$\Delta c = \sum_{j} A_{cj} \cos(\chi_j(t) - \phi_{cj}) \tag{6}$$

where:

- j index for tidal constituent ($j = 1,...,342$ for the HARDISP procedure)
- A_{cj} amplitude of the response for chosen location
- $\chi_j(t)$ astronomical argument in time for the tide
- ϕ_{cj} phase of the response for chosen location

When using relative positioning methods, low spatial variability of the displacements generated due to ocean tide movements causes elimination of the most of its influence during observation differentiation. Absolute positioning methods, like PPP, enable observing the influence of OTL as it directly influences the observed range and is mapped to result coordinates.

3. METHODOLOGY

Analysis of OTL influence on PPP method was performed basing on 24 globally distributed permanent stations (Fig. 1). They were chosen as a subset of the IGS core network considering their distribution, quality and continuity of observations.

Fig. 1. Permanent stations used in the analysis and influence of application of tides model on the results (RMS value improvement for 4 hour interval).

Each of the stations' position was obtained using the gLAB, an open-source PPP software (Hernandez-Pajares, et al., 2010). The current version does not contain the OTL model and thus it was implemented and added to the package by the authors according to the procedure presented in Section 2. Each calculation was performed twice, with and without application of the OTL model. Calculations contained observations from 50 consecutive days between 01.01.2012 and 19.02.2012. The observation set was preprocessed so that files for durations of 24, 12, 8, 6, 4, 3, 2 and 1 hours were generated resulting in 1200, 2400, 3600, 4800, 7200, 9600, 14400 and 28800 performed calculations for each period, respectively. Errors were obtained through comparison of the results to reference coordinates of the stations. Outliers were detected using the Chauvenet's Criterion (Taylor, 1996) and removed.

Root mean square (RMS) error was used as a quality indicator. For each single processing execution, differences between the reference and calculated coordinate were determined separately for horizontal and vertical components. The RMS for n differences ($m_1, m_2, ..., m_n$) assigned to each of the observation duration was calculated by:

$$RMS_i = \sqrt{\frac{m_1^2 + m_2^2 + ... + m_n^2}{n}} \tag{7}$$

These RMS values for the results obtained with and without the OTL model were used as an indicator of the OTL influence. The relative value (in %) was obtained by dividing the absolute value by mean of the values with and without the OTL model (see Table 2).

The influence of the OTL model on mean convergence time and standard deviation of the convergence time was obtained by analysing all the 24 hour execution results with and without the OTL model for convergence values between 1 and 10 cm. Subtraction of the mean and standard deviation with and without the OTL model was used to analyse the influence of the OTL model on the convergence (see Fig. 6).

4. RESULTS

Station GUAM (see Figure 1, red square) was chosen for presentation of OTL influence on PPP positioning of single station. The influence is big for this station. The respective displacements for the whole analysed period, single week and single day are presented in Figure 2. For each component the loading is calculated according to Eq. 6. Tidal coefficients for this particular location are presented in Table 2. Each of the Up, West, South components contains 11 pairs of amplitudes and phases.

The displacements of up to 4cm can be observed for the Up (radial) component while horizontal components reach 1 cm level. As expected, the harmonic nature of the displacements is observed. Monthly, diurnal and semidiurnal periods are distinguishable (Fig. 2).

A station displacement directly influences the modeled range between a receiver and GNSS satellite. All components are projected to receiver-satellite vector and applied to distance value. Fig. 3a presents displacement values and their influence on the modeled distance for single G04 satellite during day 08.01.2012. Additionally, elevation of the observed satellite was presented (Fig. 3b). Positioning results for single calculation are presented in Figure 3d. The change for each of the components corresponds to cumulative tidal displacement.

Table 1. Amplitudes and phases for 11 main tidal waves for the location of the station GUAM.

	M2	S2	N2	K2	K1	O1	P1	Q1	MF	MM	SSA
A_u[mm]	10.29	1.91	2.55	0.3	15.24	10.22	5.01	1.97	0.86	0.56	0.49
A_w[mm]	4.89	2.48	0.92	0.65	1.04	0.93	0.35	0.19	0.04	0.02	0.01
A_s[mm]	0.29	0.57	0.13	0.2	0.83	0.58	0.27	0.11	0.05	0.02	0.02
$\varphi_u[^0]$	95.8	75.9	77.1	41.8	-117.9	-135.2	-118.3	-140.6	-163.3	-167.6	-177.4
$\varphi_w[^0]$	-47.9	-23	-52.8	-28.4	178.7	149.2	179.5	138	-68.7	-120	-167
$\varphi_s[^0]$	70.2	122.7	-149.6	107.2	110.4	109.8	110.2	106.7	-7.8	-0.9	0.6

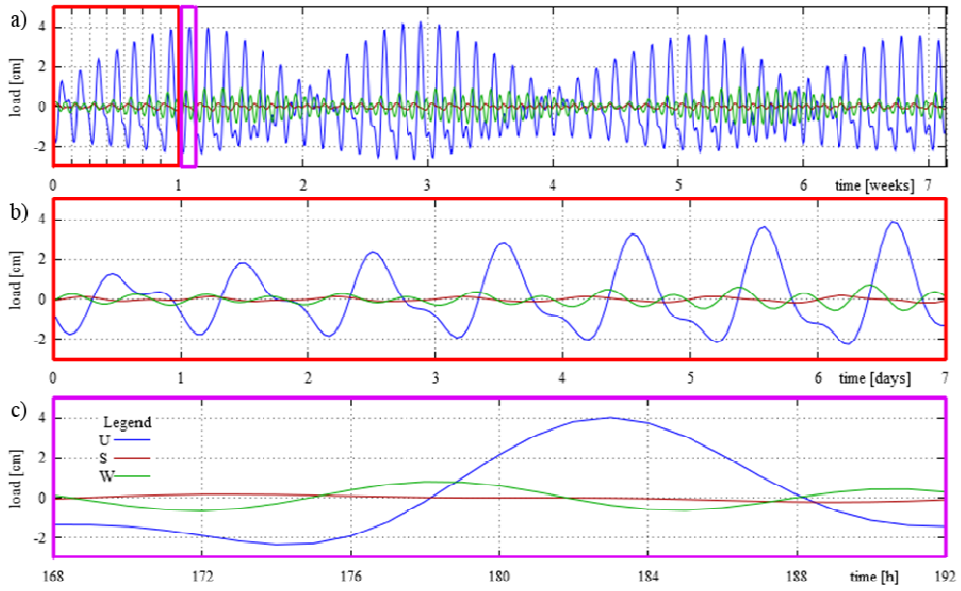

Fig. 2. Displacement for the GUAM station in time for: 50 days (a), single week (b) and for single day (c).

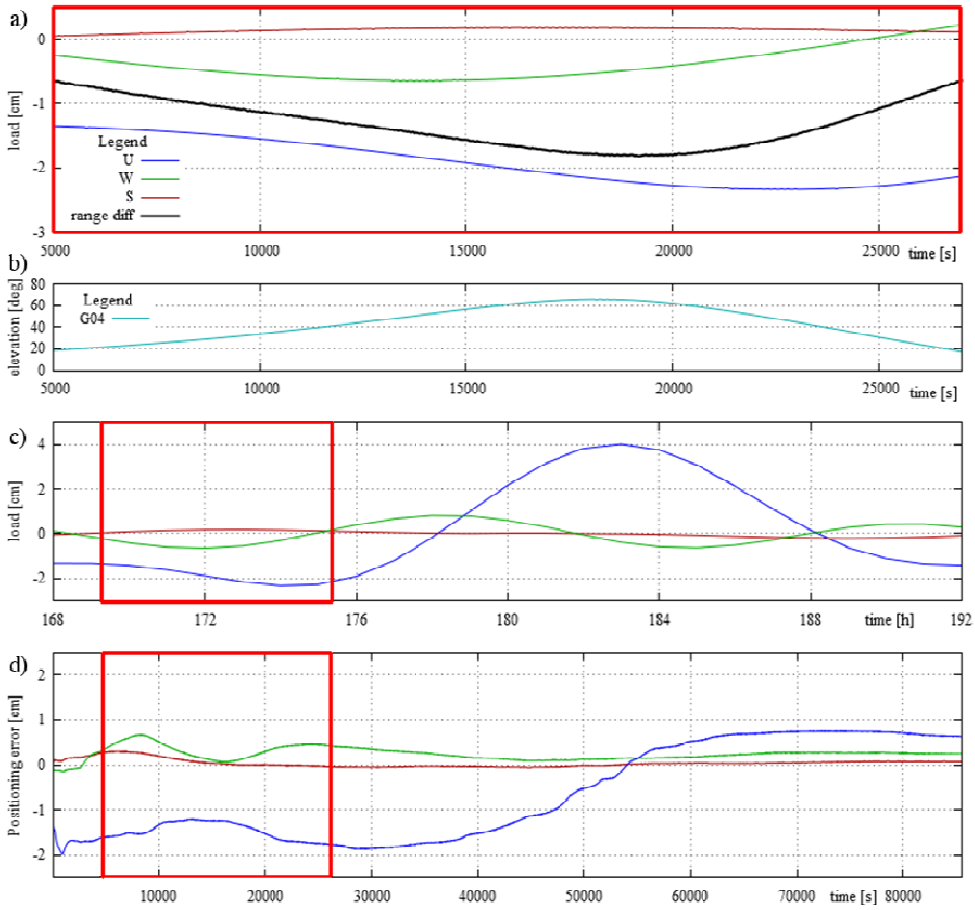

Fig. 3. Influence of ocean tidal displacement on receiver-satellite modeled range based on satellite G04. Modeled range (a) for satellite with elevation in (b), load value (c) and static positioning results error difference (d) for day 08.01.2012 and the GUAM station.

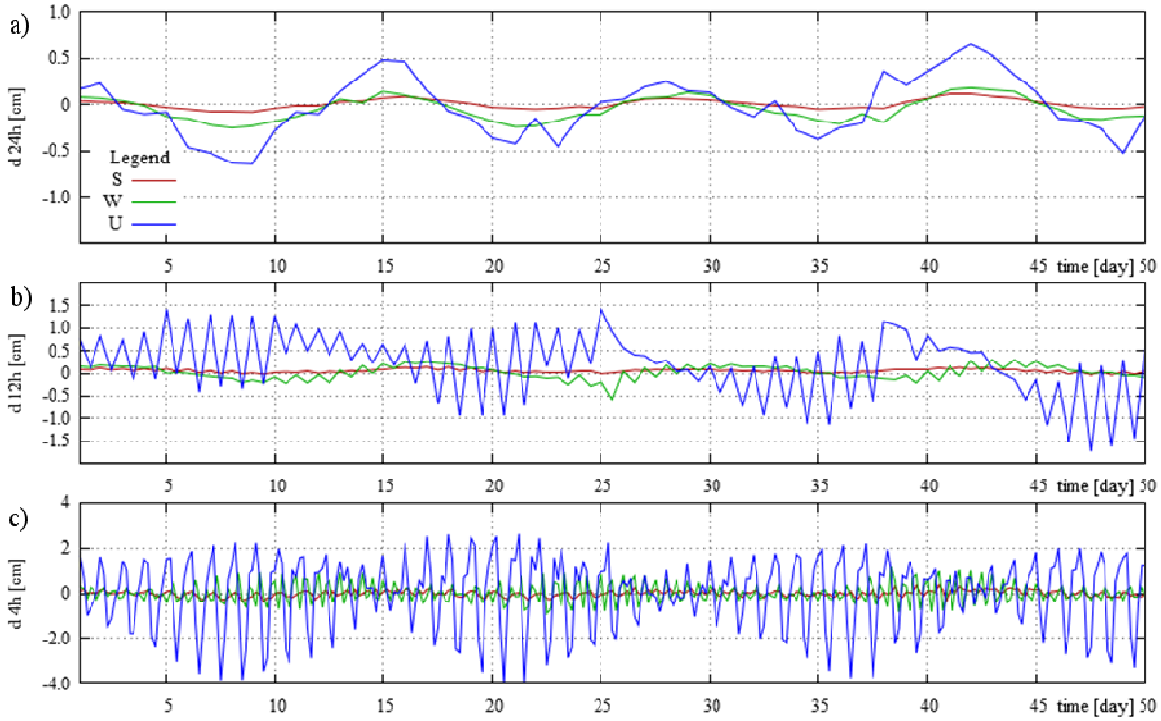

Fig. 4. Impact of the station GUAM's OTL model on vertical component time series for 24 (a), 12 (b) and 4 (c) hour interval.

Time series for the impact of the OTL model on positioning error with regard to catalogue coordinates in days is presented in Figure 4. Ocean tides loading plays minor role in the final coordinates. For the analysed station and 24 interval, difference reaches maximum value of 7 mm during day 42. With observation length of 24 hours the difference corresponds to averaged influence of tidal loading. This results in small final differences in coordinates. The RMS values are improved by about 2-3% for each component (see Table 2). The effect of OTL does not play dominant role in the 24h time series, however, it is observable for the applied model. The increase of OTL influence is proportional to decrease of observation time. As the observation sets are fixed to the time of day, similarly to the OTL, the periodic influence is distinguishable (Fig. 4). The difference between two chosen executions can reach 1, 2 and 6 cm for 24, 12 and 4 hours interval, respectively. For time shorter than 24 hours the difference exists between executions during a day. Thus, omitting OTL influence may lead to differences of several centimeters even for measurements during the same day.

Table 2 presents the results (for the station GUAM and for all other analysed stations) of the analysis for several observation lengths, with statistical parameters of the time series and influence of OTL as absolute and relative values. For the GUAM station the improvement in RMS error reaching up to 8 mm can be observed for height component. In addition, when observing the results with the OTL model applied, the dispersion of the results is decreased. For time periods less than 24 hours the improvement increases. Relative values of the improvement reach up to 20% for RMS value of height component (for 8 hour interval). Lengths between 12 and 3 hours show good proportion between the final accuracy and influence of OTL. The relative influence shows up and remains above 10% for those times. Basing on the results it can be stated that for observation periods up to 12 hours and model quality of several centimeters and better, OTL effects should be considered. Further decreasing the observation lengths deteriorates the accuracy so that the influence of OTL effects does not play significant role.

By taking all the stations into consideration the application of the OTL model for PPP calculation improves the RMS accuracy of the results. The improvement for horizontal components does not exceed 3% for relative or 0.4 mm for absolute values. For the vertical component the improvement goes from 0% for 24 hour interval, through 3% (for 12 and 1 hours) to 9% (for 6 and 4 hours). Lower values than for the GUAM station were expected as for the analysis stations with lower influence of OTL effects were included.

Table 2. Improvement in RMS for station GUAM and all stations after modeling the OTL effects.

	T [h]	**24**	**12**	**8**	**6**	**4**	**3**	**2**	**1**
Absolute	lat [mm]	0.1	0.2	0.1	0.1	0.2	0.1	0	0.1
GUAM	lon [mm]	0.3	-0.1	0	-0.2	0.2	0	-0.3	-0.6
	h [mm]	0.5	4.5	7.3	7.4	6.2	6.1	4.4	3.2
Relative	lat [%]	3	4	2	1	1	0	0	0
GUAM	lon [%]	3	0	0	-1	1	0	0	-1
	h [%]	2	13	19	15	11	10	5	2
Absolute	lat [mm]	0.0	-0.1	0.1	0.2	0.2	0.2	0.3	0.2
ALL	lon [mm]	0.2	0.3	0.3	0.3	0.2	0.4	0.2	-0.2
	h [mm]	0.0	0.4	1.3	1.8	2.2	2.1	2.0	1.6
Relative	lat [%]	0	-1	2	2	2	2	2	1
ALL	lon [%]	3	3	3	2	1	2	1	0
	h [%]	0	3	7	9	9	7	5	3

The results presented in Table 2 were estimated by cumulating all the results, disregarding the phase of ocean loads for which the calculation was performed. And so the statistics are flattened by time averaging where the loads were at extreme values with minor loads. In addition time of day can influence the quality of the PPP calculation. Wang (2013) correlates the daily variability of positioning quality with accumulative precipitation. In this paper authors show amount of the OTL model impact on positioning quality for the GUAM station. Length of 3 hours was used for the analysis which is assumed to be a good tradeoff between the resolution of the analysis (8 periods for each day) and the quality of the solution (58 mm RMS and 10% of OTL influence).

Figure 5 shows statistical parameters of mean value, standard deviation and RMS error for different parts of day with the interval of 3 hours, based on the result of the GUAM station. Since the ocean tide periods are correlated with time of day, the improvement corresponds to value of tide load presented in Figure 2-c scaled depending on amplitude of the load during the day and averaged. Mean values are less dissipated when the OTL model is applied. When comparing mean value change of height component with average radial tidal displacement it can be stated that the average displacement is projected directly to final coordinate.

Graphical presentation of OTL influence on RMS values based on 4 hour intervals and whole set of stations is included in Figure 1. The improvement is calculated by subtracting the RMS values calculated for single station, and whole processing period of 50 days, with and without the OTL model. The maximum improvement reaches about 1 cm.

The convergence time analysis was performed based on the results of 24 hour calculation. The values for the convergence without the OTL model are presented in previous research (Kalita et al., 2014). The improvement of the convergence time by applying the OTL model is presented in Figure 6. For the accuracy of about 5 cm the convergence time is improved by over 800 seconds and the standard deviation is improved by about 1000 seconds. Thus for the order of 5 cm and more accurate analysis the OTL modeling plays important role as total measurement time can be reduced while preserving the assumed accuracy.

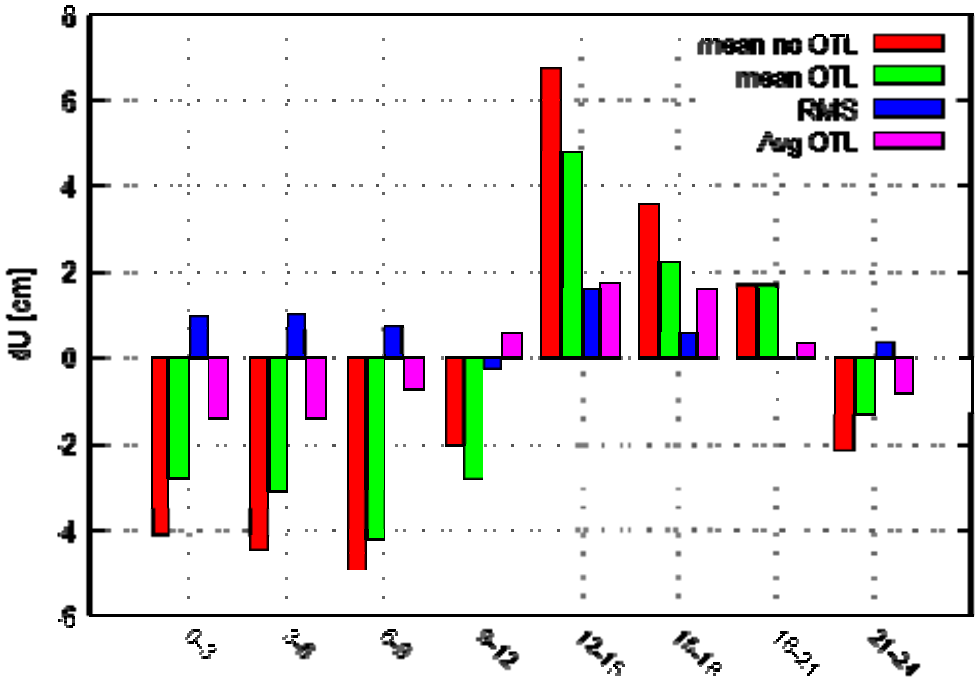

Fig. 5. Analysis of daily variability of PPP solution for height component, RMS and the OTL model average height displacement for 3 hour periods during the day, GUAM station.

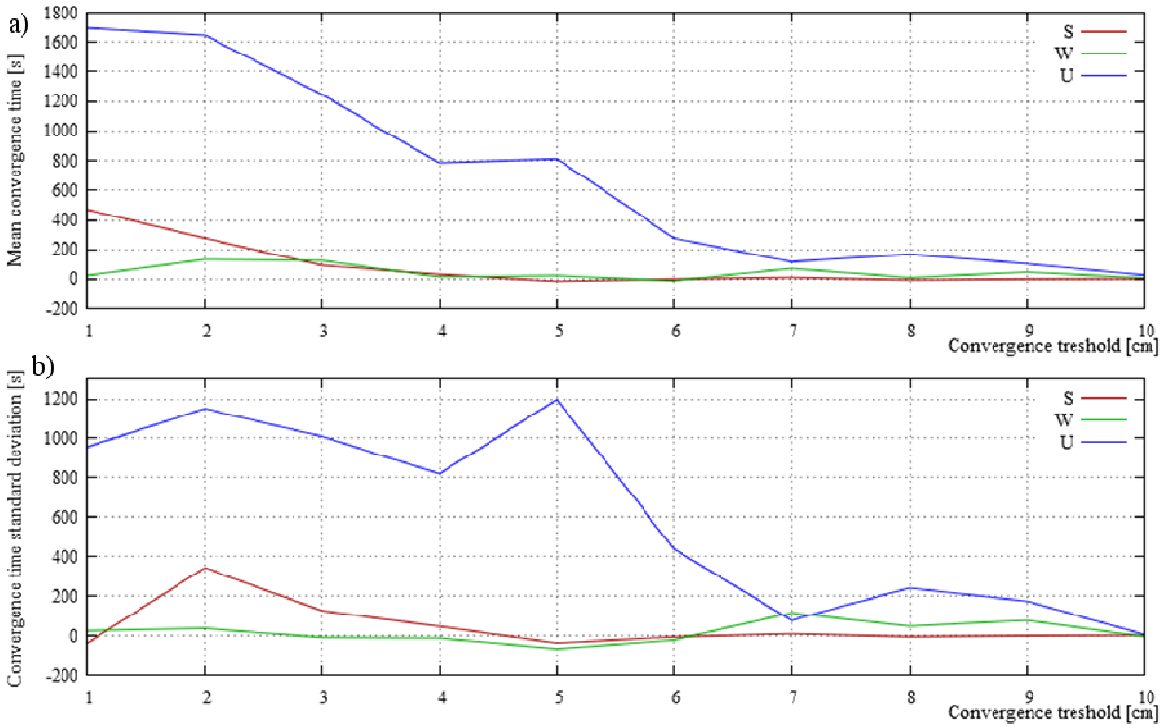

Fig. 6. Mean (a) and sigma (b) improvement of the OTL model application on PPP convergence.

5. INFLUENCE OF OCEAN TIDES LOADING IN POLAND

The influence of the OTL reaches its maximum for stations close to large masses of oceans and thus expected loading influence in Poland is small. For the analysis, 5 points distributed over Poland were analysed basing on procedure described in Section 2. ASG-EUPOS stations' positions were used for this purpose (Bosy et al., 2008); in particular: WLAD, KUTN, ZYWI, MIES, BPDL. Loads for horizontal and vertical components were generated for period of 50 days, between 01.01.2012 and 19.02.2012 (see Section 3).

Figure 7 presents loads for single station placed in central Poland (KUTN) calculated based on the HARDISP procedure (see Section 2). Amplitude values are between single mm and about 8 mm. Figure 9b presents loads for one day when the influence was the highest during the 50 day period. Vertical component does not stand out as much as for the GUAM station analysed in Section 4. The loads for horizontal components show direction of water masses that cause the load.

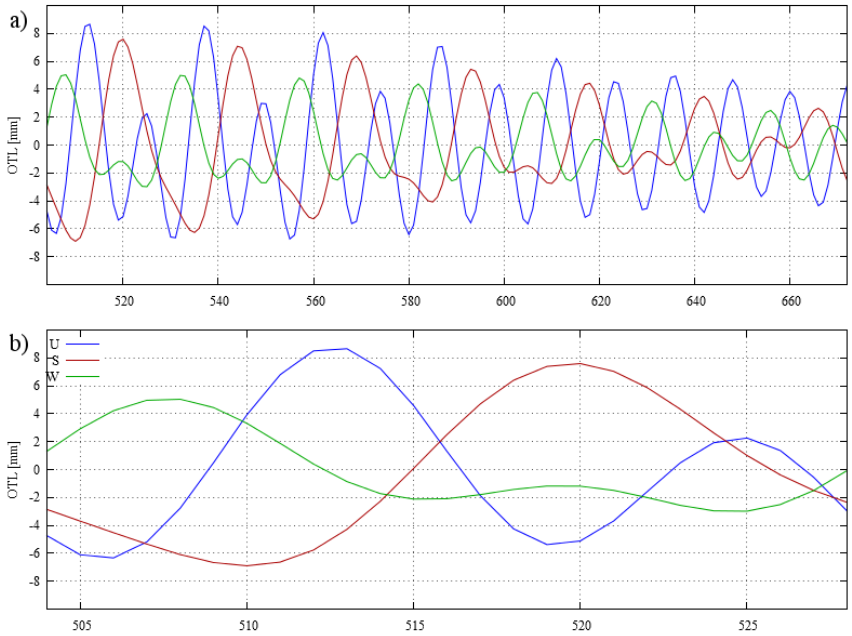

Fig. 7. Loads for position of KUTN station for 4th week (a) and for day 22 (b) when the amplitudes are the highest.

The extreme values were compared for all stations as a draft attempt to determine the spatial variability of the loads (Table 3). Large, over 2 mm difference is observed for radial component between north (WLAD) and south (ZYWI) part of Poland. Variability of over 1 mm between east (BPDL) and west (MIES) parts of Poland stands out. Differences for the rest of the analysed data does not go beyond 0.5 mm.

Table 3. Extreme values of loads for chosen stations in Poland.

		Load for station [m]		Load for station [m]			
load direction	hour	ZYWI	KUTN	WLAD	BPDL	KUTN	MIES
d_u[mm]	513	9.3	8.7	7.1	8.5	8.7	8.9
d_s[mm]	520	7.4	7.6	7.9	7.5	7.6	7.8
d_w[mm]	507	5.0	5.0	5.1	4.4	5.0	5.7

During positioning values of loads get averaged and thus result biases will be smaller than maximum displacements. However for absolute positioning methods as PPP, OTL models should be included when the sub-centimeter accuracy and short observation intervals are considered. When comparing the analysed GUAM station and the OTL model in Poland by proportion between the extreme OTL and relative improvement, the 8mm OTL value results in improvement up to 4%. This was confirmed by performing the comparative calculation according to the methodology from Section 3 using BOR1 permanent station. The highest improvement of 0.5 mm or 3.7% in the RMS value was observed for height component and 4 hour interval.

6. CONCLUSIONS

Although influence level of OTL is location dependent, the analysis performed on several globally distributed stations, taking into consideration stations where the influence is high as well as stations with minor influence, resulting in general averaged influence of the OTL effect on PPP positioning. In addition the influence for a station where the OTL effect is high is analysed. In addition a draft attempt to show the OTL influence for area of Poland is done.

As the PPP is an absolute method, the loads cumulate and transfer nearly directly to the positioning solution. Consequently, for short observation intervals and small loads the application of the model does not play an important role. After the solution converges to accuracy corresponding to amplitudes of the loads, the relative influence increases. For the GUAM station the maximum influence for the radial component reached over 7 mm RMS (for interval 8h and 6h) or 19% (for 8 hours interval). For the intervals of 24 hours most of the OTL radial displacement is averaged. The horizontal OTL displacement is typically small rarely exceeding 3%. In general, for absolute positioning methods, like PPP, the OTL model should be included when the centimeter (or sub-centimeter for Poland) accuracy and short observation intervals are considered.

REFERENCES

Abdel-salam M. (2005) Precise Point Positioning Using Un-Differenced Code and Carrier Phase Observations. *PhD Thesis*, University of Calgary.

Bisnath S., Gao Y. (2009) Current State of Precise Point Positioning and Future Prospects and Limitations, *Observing our Changing Earth. International Association of Geodesy Symposia 133*, ed. Sideris M. G., Berlin, Springer-Verlag, 615–623.

Blewitt G. (2003) Self-consistency in reference frames, geocenter definition, and surface loading of the solid Earth, Journal *of Geophysical Research: Solid Earth*, Vol. 108, No. B2.

Bosy J., Oruba A., Graszka W., Leończyk M., Ryczywolski M. (2008) ASG-EUPOS densification of EUREF Permanent Network on the territory of Poland, *Reports on Geodesy*, Vol. 85, No. 2, 105-111.

Dodson A. T. (1921) The Harmonic Development of Tide-Generating Potential, *Proceedings of the Royal Society of London. Series A, Containing Papers of a Mathematical and Physical Character*, Vol. 100, No. 704, 305-329.

Ebner R., Featherstone W. E. (2008) How well can online GPS PPP post-processing services be used to establish geodetic survey control networks?, *Journal of Applied Geodesy*, Vol.2, No. 3. 149–157

Farrell W. E. (1972) Deformation of the Earth by Surface Loads, *Reviews of Geophysics and Space Physics*, Vol. 10, No. 3, 761-797.

Fu Y., Freymueller J. T., van Dam T. (2011) The effect of using inconsistent ocean tidal loading models on GPS coordinate solutions, Journal of Geodesy, Vol. 86, No. 6, 409-421.

Griffiths J., Ray J. R. (2009) On the precision and accuracy of IGS orbits, *Journal of Geodesy* Vol. 83, No. 3–4, 277–287.

Hernandez-Pajares M., Juan J. M., Sanz J., Ramos-Bosch P., Rovira-Garcia A., Salazar D., Ventura-Traveset J., Lopez-Echazarreta C., Hein G. (2010) The ESA/UPC GNSS-Lab tool (gLAB): an advanced multipurpose package to process and analyse GNSS data, *5th ESA Workshop on Satellite Navigation User*, Noordwijk , The Netherlands, 2010.

Hofmann-Wellenhof B., Lichtenegger H., Wasle E. (2008) GNSS – Global Navigation Satellite Systems. Springer-Verlag, Wien.

IERS Conventions (2010) Petit G., Luzum B. , Verlag des Bundesamts für Kartographie und Geodäsie, Frankfurt am Main.

Kalita J. Z., Rzepecka Z., Szuman-Kalita I. (2014) The application of Precise Point Positioning in Geosciences, *Proc. of the 9th International Conference Environmental Engineering*, Vilnius 2014.

Kouba J., Héroux P. (2001) GPS precise point positioning using IGS orbit products, *Physics and Chemistry of the Earth, Part A: Solid Earth and Geodesy*, Vol. 26, No.6–8, 573–578.

Kouba J. (2009) A Guide to using International GNSS Service (IGS) products, ftp://ww.igs.org/igscb/resource/pubs/UsingIGSProductsVer21.pdf (accessed Sep 2014).

Landau H., Chen X., Klose S., Leandro R., Vollath U. (2009) Trimble's RTK and DGPS Solutions in Comparison with Precise Point Positioning, *Observing our Changing Earth. International Association of Geodesy Symposia 133*, ed. Sideris M. G., Berlin, Springer-Verlag, 615–623.

Leandro R. F., Santos M. C., Langley R. B. (2011) Analyzing GNSS data in precise point positioning software, *GPS Solutions,* Vol. 11, No. 1, 1–13.

Lyard F., Lefevre F., Letellier T., Francis O. (2006) Modelling the global ocean tides: modern insights from FES2004, *Ocean Dynamics*, Vol. 56, 394-415.

Stępniak K., Wielgosz P., Paziewski J. (2012) Badania dokładności pozycjonowania techniką PPP w zależności od długości sesji obserwacyjnej oraz wykorzystanych systemów pozycjonowania satelitarnego [Analysis of PPP accuracy depending on observing session duration and GNSS systems used], *Biuletyn WAT* [*Military University of Technology Bulletin*], Vol. 61, No. 1, 429–450.

Taylor J. R. (1996) *An Introduction to Error Analysis: The Study of Uncertainties in Physical Measurements*. Sausalito: University Science Books.

Wang G. Q. (2013) Millimeter-accuracy GPS landslide monitoring using Precise Point Positioning with Single Receiver Phase Ambiguity (PPP-SRPA) resolution: a case study in Puerto Rico, *Journal of Geodetic Science*, Vol. 3, No. 1, 22–31.

Zumberge J. F., Heflin M. B., Jefferson D. C., Watkins M. M., Webb F. H. (1997) Precise Point Processing for the Efficient and Robust Analysis of GPS Data from Large Networks, *Journal of Geophysical Research: Solid Earth*, Vol. 102, No. B3, 5005–5017.

Received: 2014-10-13,
Reviewed: 2015-04-14, by W. Kosek,
Accepted: 2015-04-20.